Applied Surface Science 436 (2018) 934–940

Contents lists available at ScienceDirect

Applied Surface Science

journal homepage: www.elsevier.com/locate/apsusc

Full Length Article

Microwave assisted synthesis of camellia oleifera shell-derived porous carbon with rich oxygen functionalities and superior supercapacitor performance

Jiyuan Liang[a,c], Tingting Qu[a], Xiang Kun[a], Yu Zhang[a], Shanyong Chen[a], Yuan-Cheng Cao[c], Mingjiang Xie[a,b,**], Xuefeng Guo[a,*]

[a] Key Lab of Mesoscopic Chemistry MOE, School of Chemistry and Chemical Engineering, Nanjing University, Nanjing 210023, China
[b] Hubei Key Laboratory for Processing and Application of Catalytic Materials, Huanggang Normal University, Huanggang 438000, China
[c] Key Lab of Optoelectronic Chemical Materials and Devices, Ministry of Education, Jianghan University, Wuhan 430056, China

ARTICLE INFO

Article history:
Received 12 May 2017
Received in revised form
23 November 2017
Accepted 17 December 2017
Available online 18 December 2017

Keywords:
biomass
microwave carbonization/activation
porous carbon
electrochemical-active oxygen
supercapacitor

ABSTRACT

Biomass-derived carbon (BDCs) materials are receiving extensive attention as electrode materials for energy storage because of the considerable economic value offering possibility for practical applications, but the electrochemical capacitance of BDCs are usually relatively low resulted from limited electric double layer capacitance. Herein, an oxygen-rich porous carbon (KMAC) was fabricated through a rapid and convenient microwave assisted carbonization and KOH activation of camellia oleifera shell. The obtained KMAC possesses three-dimensional porous architecture, large surface area (1229 m^2/g) and rich oxygen functionalities (C/O ratio of 1.66). As the electrode materials for supercapacitor, KMAC exhibits superior supercapacitive performances as compared to the activated carbon (KAC) derived from direct carbonization/KOH activation method in 2.0 M H_2SO_4 (315 F/g *vs.* 202 F/g) and 6.0 M KOH (251 F/g *vs.* 214 F/g) electrolyte due to the rich oxygen-containing functional groups on the surface of porous carbon resulted from the developed microwave-assisted carbonization/activation approach.

1. Introduction

With the development of high-performance energy storage technology, supercapacitors have received great attention because of their high power capability, long cycle life, low cost and environmental friendliness. [1,2] Supercapacitor has been considered to be a promising candidate for energy storage devices. According to the charge-storage mechanism, supercapacitorsare classified into electric double layer capacitor (EDLC) and pseudocapacitor. EDLC usually uses carbon-based active materials as their electrode and store charges based on the electrostatic adsorption of charge separated ions on the surface of active materials. Pseudocapacitor with transition metal hydroxides/oxides [3–6] and conductive polymers (such as polypyrrole, polyaniline, *etc.*) [7,8] as the active materials storages electric energy by fast and reversible redox reactions. The capacities of pseudocapacitor are usually ten to one hundred times higher than that of EDLC, but the rate performance and cycling life are usually poor due to their inferior conductivity and instable microstructure. Whereas, EDLCs can perform ultrahigh power density and excellent cycling life since the adopted carbon-based electrode materials owns stable microstructure/morphology.

Among carbon materials with various morphologies, porous carbon are the most commonly used active materials for supercapacitor due to their unique features of porous structure, tunable pore size, controllable surface area, ease of synthesis [9–12]. Considering from the practical application, biomass derived carbons (BDCs) have attracted wide research interests as a promising electrode material since biomass is abundant, renewable and low cost. To date, various biomasses have been adopted as starting materials towards the fabrication of porous carbon materials. [13–17] However, the electrochemical capacitance of the BDCs-based electrodes are usually relatively low (usually < 300 F/g in aqueous electrolytes) resulted from limited EDLC. In order to further enhance the capacitance of the electrodes, efforts have been devoted to introducing pseudocapacitive functionalities into the carbon substrates by incorporating heteroatoms-containing (e.g. O, N, P, S) functional groups.[18–20] The heteroatoms-containing

* Corresponding author.
** Corresponding author at: Key Lab of Mesoscopic Chemistry MOE, School of Chemistry and Chemical Engineering, Nanjing University, Nanjing 210023, China.
E-mail addresses: xiemingjiang@hotmail.com (M. Xie), guoxf@nju.edu.cn (X. Guo).

https://doi.org/10.1016/j.apsusc.2017.12.142
0169-4332/

functional groups not only can modify the surface wettability, but also can enhance the capacitance through Faradaic reaction with electrolyte ions.[21,22] Among heteroatoms modified carbon materials, carbons with rich oxygen functionalities offers a promissing applications in energy storage and conversion.[23–26] For example, Anjos *et al.* [27] reported that quinone-modified onion-like carbon achieved a higher capacitance up to 264 F g^{-1} than that of the unmodified onion-like carbon (30 F g^{-1}) in 1.0 M H_2SO_4 electrolyte due to the Faradic reaction (-C=O + H^+ + e- ↔ -C-O-H) of quinone groups with the electrolyte, indicating that the capacity performance of carbon materials can be greatly improved through introducing electroactive oxygen groups.

However, to date, functional carbons are usually prepared by post-treatment of crude carbon with reactive sources (e.g. ammonia) or by direct pyrolysis of rich heteroatom-containing precursors at high temperature. However, high temperature post-treatment or pyrolysis does not favor the retention of heteroatom-containing group in carbon materials and thus the traditional approach derived functional carbons usually owns very low doping amount of heteroatoms (<10 %). In this regard, there is a critical need to develop an efficient low-temperature carbonization method. Recently, microwave-assisted carbonization has been proved to be an effective towards the preparation of carbonaceous materials. For example, Ji *et al* reported the preparation of activated carbons by microwave heating method (at power of 3 kW for 6-8 min) and found that the prepared activated carbons by microwave heating show lower content of oxygen containing groups than that prepared via direct conventional heating method.[28]

Herein, porous carbon with rich oxygen functionalities (KMAC) was prepared by microwave-assisted carbonization and KOH activation of camellia oleifera shell (COS). Camellia oleifera shell, a kind of biomass waste of oil crop in the south of China, owns high oxygen content of 44% [29] and offers a promising raw material for producing oxygen-rich porous carbon. In our strategy, the collected COS was washed and dried prior to pre-carbonization. The dried COS was pre-carbonized at 400 °C and then activated by KOH with various weight ratios by microwave treatment. After removal of the activated reagent of KOH, the obtained KMAC possesses three-dimensional porous architecture, large surface area (1229 m^2/g) rich electrochemical-active oxygen functionalities (C/O ratio of 1.66) and exhibits superior supercapacitive performances as compared to the activated carbon (KAC) derived from direct carbonization/KOH activation method. In our approach, the obtained KMAC by microwave-assisted carbonization possesses higher oxygen content than that obtained by direct conventional carbonization, contrary to the reported results [28], which can be attributed to the low achieved treating temperature due to the low input power (600 W) and short microwave treatment time (3 min) adopted in our approach. The low treating temperature and short treating time may reduce the pyrolysis of camellia oleifera shell and retain higher content of oxygen containing groups. Since the microwave heating treatment [30] possesses the unique characters of rapid heating and timesaving, it can be expected that the functional groups in biomass could be massively preserved after microwave-assisted carbonization at low power and hence the supercapacitive performance of the derived carbon electrode materials would be enhanced to a higher level.

2. Experiment

2.1. Synthesis

The collected camellia oleifera shell (COS) was firstly washed with distilled water and dried at 80°C for 12 h. The dried COS was ground into pieces and pre-carbonized at 400°C for 1.0 h under Ar atmosphere to obtain the as-prepared char. Then the char was soaked in 6.0 M KOH solution ($Weight_{KOH}/Weight_{char} = 3$) to obtained the KOH/char composite. The KOH/char composite was transferred into ceramic crucible and placed in the microwave oven to undergo a microwave treatment for 3 min at power of 600 W. After microwave treatment, the obtained sample was washed with 1.0 M HCl solution and then thoroughly washed with deionized water. As comparison, the KOH/char composite was treated by a direct high temperature carbonization/activation method at 800 °C for 3 h under Ar atmosphere. The resulting carbons by microwave treatment and direct carbonization method were denoted as KMAC and KAC-800, respectively.

2.2. Characterizations

The X-ray diffraction (XRD) pattern of the product was recorded on Philips X'Pro diffract meter using Cu Kα radiation (λ =1.5406 Å). Scanning electron microscopy (SEM) images were taken by a field-emission scanning electron microscope (Hitachi S-4800). Nitrogen sorption analysis was carried out using a Micromeritics ASAP2020 analyzer at 77 K. The Brunauer-Emmett-Teller (BET) method was utilized to calculate the specific surface areas. The pore size distribution plots were analyzed from the desorption branch of the isotherms based on the Barrett-Joyner-Halenda (BJH) model. Elemental analysis was performed by a vario EL-II. X-ray photoelectron spectroscopy (XPS) was recorded on ESCALB MK-II (VG) X-ray photoelectron spectroscopic instrument. All binding energies (BEs) were referenced to the C1s peak at 284.6 eV. FTIR spectra were recorded on a VECTORTM 22 spectrometer.

2.3. Electrochemical measurements

All the electrochemical measurements were carried out using a CHI660D electrochemical workstation at room temperature. The electrode was prepared by pressing a mixture of 85 wt. % active material, 10 wt.% acetylene black and 5 wt. % Polytetrafluoroethylene (PTFE) binder onto a nickel foam or stainless steel mesh and dried in a vacuum oven at 80 °C for 6 h. The mass loading of active material in each electrode was about 2.0 mg. In the three-electrode system, a platinum wire and Hg/Hg_2Cl_2 (SCE) or Ag/AgCl electrodes were used as counter and reference electrodes, respectively. 6.0 M KOH and 2.0 M H_2SO_4 were used as the electrolyte. For the test in 6.0 M KOH electrolyte, cyclic voltammograms (CV) were tested in the voltage range between -1 and 0 V. Galvanostatic charge-discharge (GDC) measurements were carried out at current densities from 0.5 to 50 A/g. For the test in 2.0 M H_2SO_4 electrolyte, CV was performed in the voltage rage 0 to 1 V. GDC tests were measured at current densities from 0.5 to 10 A/g. The specific capacitance can be calculated by the discharge curve according to the formula of $C_s = \frac{I\Delta t}{m\Delta V}$(F/g), where I is the current density (A), Δt is the discharge time (s), m is the weight of electrode material, ΔV is the potential window of discharging (V).

3. Results and discussion

3.1. Structure and morphology analysis

Fig. S1a and b shows SEM images of COS, it can be seen that the bulk COS possesses a rough and dense surface without hierarchical porous structure. As shown in Fig. S1c and d, even after pre-treatment of COS at 400 °C, the obtained pre-carbonized COS still owns a smooth surface. As Fig. 1 and b shown, after high temperature carbonization/activation treatment by KOH at 800 °C, the obtained KAC-800 owns a porous structure with some cavities and pores on the surface due to the reaction of carbon with KOH ($6KOH + C \rightarrow 2K + 3H_2 + 2K_2CO_3$) at high temperature.[31] At higher

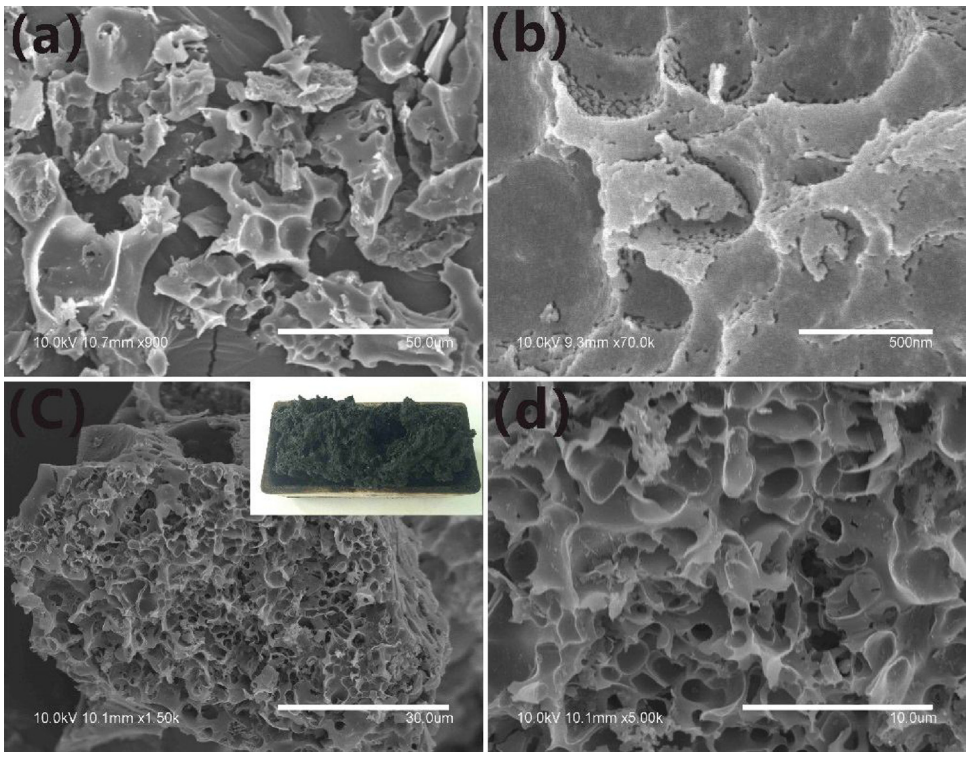

Fig. 1. SEM images of KAC-800 (a, b) and KMAC (c, d). The inset in (c) is a photograph of KMAC in a ceramic crucible after microwave carbonization/KOH activation.

temperature, K_2CO_3 and its decomposition product can further react with carbon materials as follow reactions:

$$K_2CO_3 + C \rightarrow K_2O + 2CO \quad (1)$$

$$K_2CO_3 \rightarrow K_2O + CO_2 \quad (2)$$

$$2K + CO_2 \rightarrow K_2O + CO \quad (3)$$

$$K_2O + C \rightarrow 2K + CO \quad (4)$$

Fig. 1c and d shows the SEM images of the morphology of the KMAC fabricated by microwave-assistant carbonization/activation method. It can be observed that KMAC demonstrates three-dimensional macroporous architecture with richer porosity than KAC-800, indicating that microwave heating may be favorable to the formation of porous structure than direct carbonization. Under high temperature activation condition, the pre-carbonized COS is heated through thermal conduction and/or convection. While, under microwave heating treatment, the pre-carbonized COS was fast heated by dipole rotation and ionic conduction, in which water molecular absorbed in the channels will be gasified and released in the manner of explosion, leading to the formation of porous structure and cracks. Fig. 1c-inset shows an obvious volume expansion of the microwave treated COS, implying the occurrence of the explosion resulting from the fast gasification of water. At the same time, the introduced KOH will react with carbon substrate and further

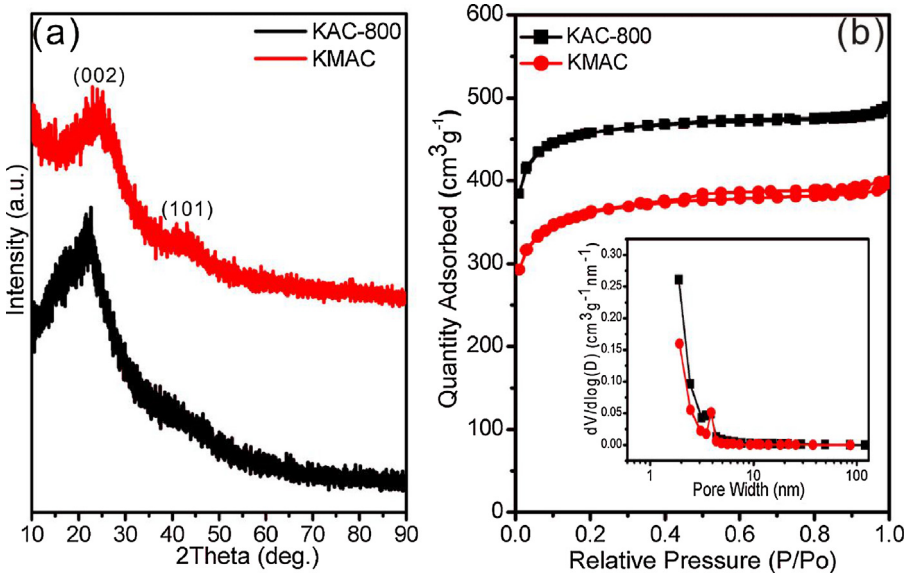

Fig. 2. (a) X-ray diffraction (XRD) patterns; (b) nitrogen sorption isotherms and pore size distribution curves (PSD inset) of KMAC and KAC-800.

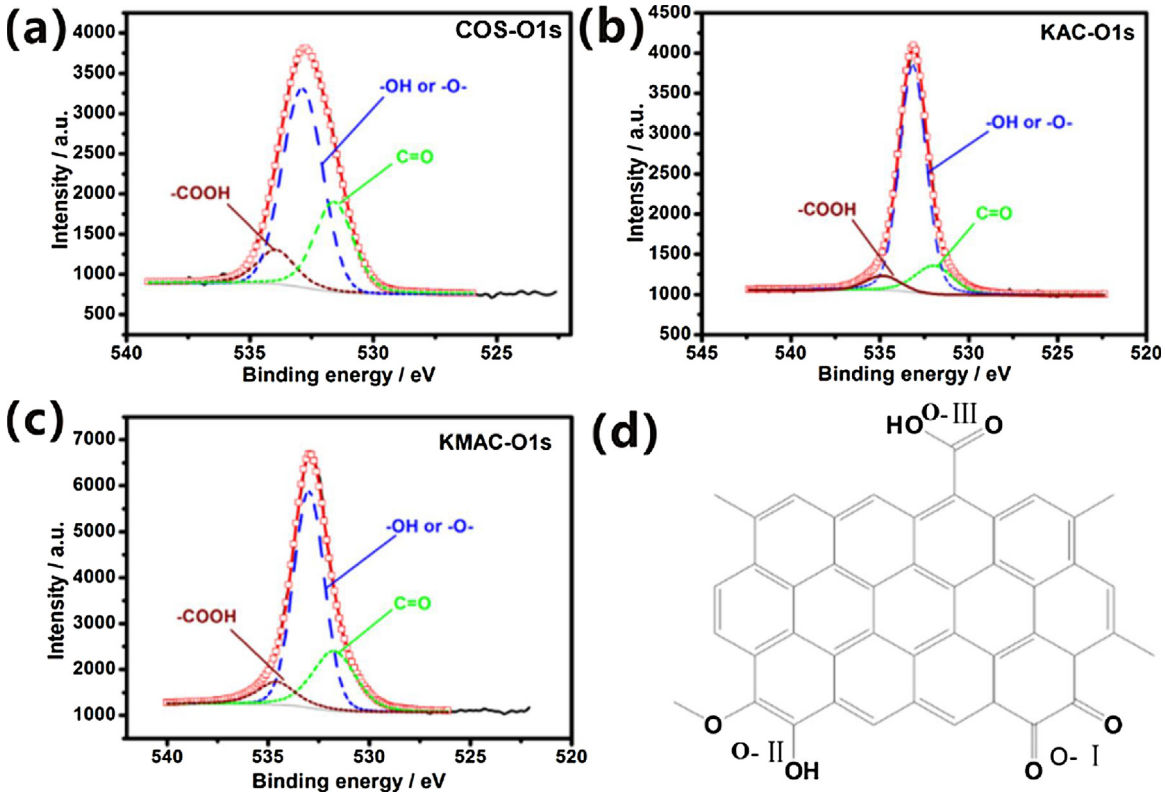

Fig. 3. High-resolution XPS spectrum of O1s peak, (a) COS, (b) KAC-800, (c) KMAC; (d) schematic illustration of oxygen species in the carbon materials.

increase the porosity of the derived carbon material. Fig. 2a shows the X-ray diffraction (XRD) patterns of KAC-800 and KMAC in wide angle region. It can be clearly seen that the two carbons both exhibit two wide peaks around 25° and 44°, corresponding to the (002) and (101) diffraction of graphitic carbon, respectively.[32] Obviously, the XRD pattern of KMAC shows similar peak intensity to that of KAC-800, implying that the microwave carbonization takes the same effect to direct carbonization.

The textural characters of the two carbons were analyzed by nitrogen sorption isotherms as shown in Fig. 2b. The nitrogen sorption isotherms of KAC is a type-I isotherms, indicative of the existence of microporous structure. For KMAC, the nitrogen sorption isotherms is also a type-I isotherms with a small hysteresis loop suggesting that the coexistence of mesopores and micropores. The pore size distribution (PSD) curves calculated from the adsorption branches (Fig. 2b inset) further reveal the microporosity of KAC-800 and KMAC. As to KMAC, the PSD curve shows a weak pore size distribution around 2.7 nm, indicative of the existence of a small fraction of mesopores. The detailed textural parameters were listed in Table S1 in supporting material. The specific surface areas are 1229 m^2/g for KMAC, 1553 m^2/g for KAC-800 and the corresponding pore volumes are 1.01 and 1.33 cm^3/g, respectively (Fig. 3).

3.2. Surface chemistry and elemental component analysis

The elemental component and surface chemistry analysis were investigated by elemental analysis (EA) and X-ray photoelectron spectrum (XPS).The chemical compositions of the samples were analyzed by elemental analysis (EA) and shown in Table 1. Obviously, KAC-800 and KMAC possess higher oxygen content than COS after activation treatment. The calculated C/O ratio of the three samples are 5.73, 3.79, and 1.66, respectively. Compared to KAC-800, the lower C/O ratio of KMAC suggests that microwave-assistant carbonization/activation method favors the oxygenic functionalities reservation. In order to investigate the type and amount of oxygen-containing functional groups on the surface of carbon materials, X-ray photoelectron spectroscopy (XPS) measurements were also carried out. Fig. 5a–c shows the O1s high-resolution XPS spectra of COS, KAC-800 and KMAC, respectively. O1s core level peaks of XPS were deconvoluted to three peaks centered at 531 eV, 532 eV and 535 eV, corresponding to three types of oxygen functional group (as Fig. 5d shown), namely -C=O quinone type group (O-I), -C-OH phenol groups and / or -C-O-C- ether groups(O-II) and carboxyl group (O-III). The detailed content of various oxygen-containing functional groups is listed in Table 1. Among the three types of oxygen species, the quinone

Table 1
Elemental analysis (EA) and XPS results of the samples.

	Elemental analysis (wt. %)				XPS analysis (at. %)		
Samples	C	H	O	C/O	C=O	—OH or —O—	—COOH
COS	72.64	14.70	12.66	5.73	11.77	59.47	28.76
KAC	77.06	2.63	20.31	3.79	14.82	78.88	6.3
KMAC	57.34	8.11	34.55	1.66	26.49	62.96	10.55

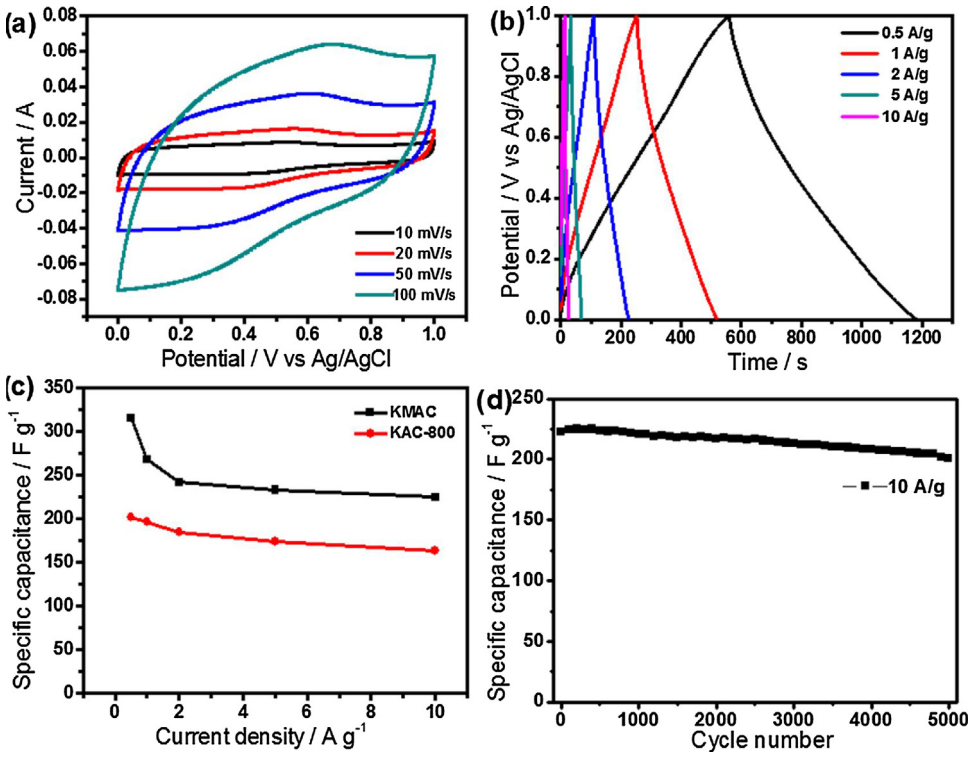

Fig. 4. Electrochemical performance of the electrodes tested in 2.0 M H_2SO_4: (a) CV plots of KMAC electrode at different scan rates; (b) galvanostatic charge-discharge curves of KMAC electrode at different current densities; (c) specific capacitance of the KMAC and KAC-800 at various current densities; (d) 5000 cycles test for KMAC at a current density of 10A/g.

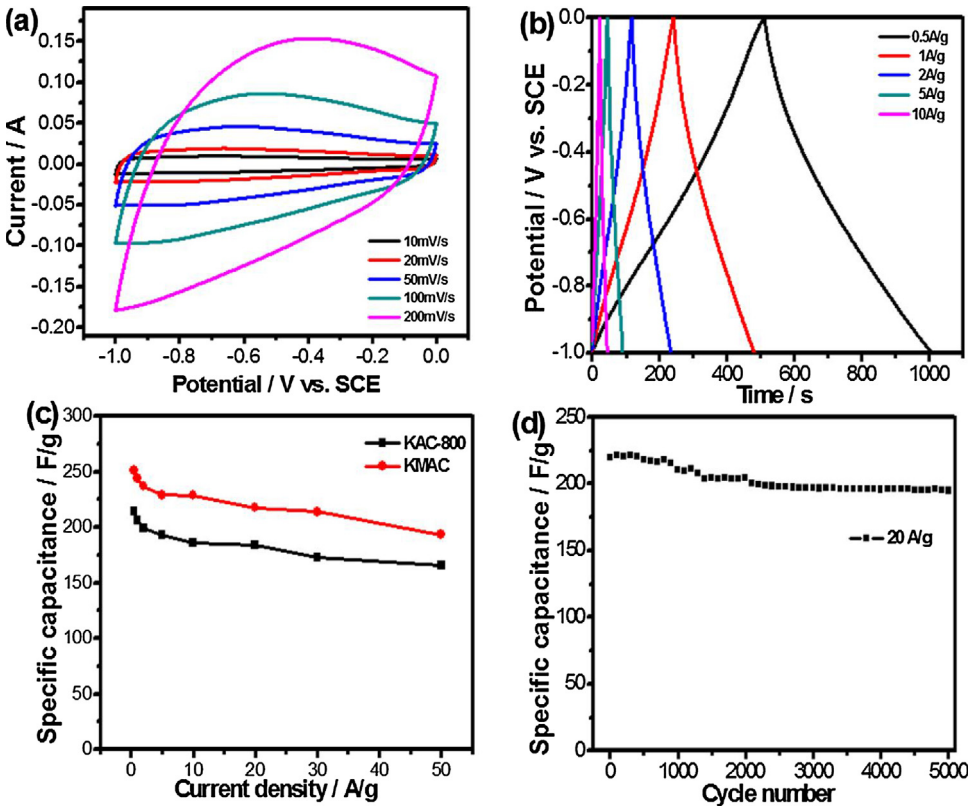

Fig. 5. Electrochemical performance of electrodes tested in 6.0 M KOH:(a) CV plots of KMAC electrode at different scan rates; (b) galvanostatic charge/discharge curves of KMAC at different current densities; (c) specific capacitance of the KMAC and KAC-800 electrode at various current densities; (d) 5000 cycles test for KMAC electrode at a current density of 20A/g.

type oxygen-containing group (-C=O O-I) is active in electrolyte by Faradic reaction (-C=O + e-↔ -C-O-) and thus could provide pseudocapacitive contributions. [21] The calculated content of O-I are 11.77 at.% for COS, 14.82 at.% for KAC-800 and 26.49 at.% for KMAC, respectively.

3.3. Supercapacitive (SC) performances of the derived activated carbons

To find the merits of the developed porous carbon as electrode for energy storage, the supercapacitive (SC) performances of the obtained KMAC (compared with KAC-800) were investigated by a three-electrode configuration in two aqueous electrolytes, i.e. 2.0 M H_2SO_4 and 6.0 M KOH electrolytes. Fig. 4 shows the SC performance of KMAC and KAC-800 in 2.0 M H_2SO_4 electrolyte. The CV plots of the KMAC (Fig. 4a) at various scan rates all exhibit a rectangular shaped pattern with a redox peak around 0.5 V, indicating the capacitance of KMAC contributed by electric double layer capacitance (EDLC) and pseudocapacitance. While, the CV plots of the KAC-800 (Fig. S2a in Supporting information) at various scan rates exhibit a rectangular shaped pattern without obvious redox signs, indicative of a typical EDLC behavior. Fig. 4b shows the galvanostatic charge/discharge curves (GDC) of KMAC at different current densities, in which the curves obviously deviate from the triangular-shaped profiles, further confirming the exsitance of pseudocapacitive behavior resulted from the possible Faradic reactions of carbonyl-containing group with acidic electrolyte (-C=O + H^+ + e-↔ -C-OH). The GDC curves of KAC-800 (Fig. S2b) at various current densities show typical triangular-shaped profiles, verifying the typical EDLC behavior of KAC-800. Fig. 4c shows the specific capacitances of the two carbons calculated from GDC curves. The calculated specific capacitances for KMAC electrode are 315, 268, 242, 233 and 225 F/g at current density of 0.5, 1, 2, 5 and 10 A/g, respectively. The initial specific capacitance of KMAC electrode can be retained 71% at 10 A g^{-1}, indicative of an excellent rate performance. Obviously, the specific capacitances of KMAC are all higher than KAC-800 (maximum capacitance of 202 F/g) at every current density and lies in high level among the recent reported various biomass derived carbon electrodes (as shown in Table S2). The superior SC performance of KMAC to KAC-800 can be attributed to the extra pseudocapacitance contribution from carbonyl-containing group. To investigate the electrochemical stability of KMAC, the galvanostatic cycling test for 5000 cycles was performed at the high current density of 10 A/g. As shown in Fig. 4d, the prepared KMAC electrode exhibits an excellent cycle stability with capacity retention of 90% after 5000 cycles.

The comparison on SC performances of KMAC and KAC-800 was also investigated by three-electrode configuration in 6.0 M KOH electrolyte. Figs. 5a and Fig. S3a show the CV curves of the KMAC and KAC-800 electrodes measured at various scan rates, respectively. It can be seen that KAC-800 exhibits a rectangular shaped CV patterns, indicating that the capacitance mainly results from the electrical double layer capacitance. However, the CV plots of KMAC electrode show rectangular shaped curve with broad humps, indicating that the capacitance derived from the electric double layer capacitance and pseudocapacitance related to redox reactions of oxygen-containing functional groups (carboxyl and phenolic groups) on the KMAC surfaces by the following depicted equations:

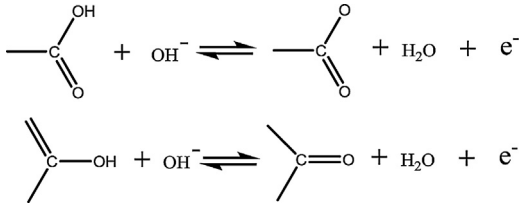

Fig. 5b displays the galavanostatic charge–dischargecurves (GDC) for the KMAC electrode at various current densities. The GDC plots show a deviation from the triangular-shaped profiles, verifing the exsitance of pseudocapacitive behavior. The specific capacitance calculated by the GDC plots of KMAC electrode is 251 F/g (at 0.5 A/g), the value is larger than that of KAC-800 electrode (214 F/g at 0.5 A/g), which can be attributed to the more amount of oxygen-containing functional groups in KMAC than that of KAC-800 offering more pseudocapacitance. It is noted that even at large current density of 50 A/g, the specific capacitance of KMAC electrode remains193 F/g, the value is 77 % of the initial capacitance, indicative of a good rate performance. The excellent rate performance of KMAC electrode can be attributed to their open and three-dimensional macroporous structure, which could serve as an ion-buffering reservoir shortening the electrolyte diffusion distance and provide more electro active surface sites for electrolyte ions. As shown in Fig. 5d, cycle stability of the KMAC electrode measured at the current density of 20 A/g has been demonstrated. After 5000 cycles, the specific capacitance of the KMAC electrode decreased from 220 to 196 F/g, with a capacitance retention of 89%, indicative of good long cycling durability.

4. Conclusion

In conclusion, an electrochemical-active oxygen functionalized porous carbon was fabricated by a microwave-assistant carbonization/activation method with biomass waste of camellia oleifera shell as starting material. The obtained porous carbon possesses three-dimensional porous architecture, large surface area (1229 m^2/g) and rich electrochemical-active oxygen functionalities (C/O ratio of 1.66). As electrode for supercapacitor, the microwave-assistant carbonization/activation method derived porous carbon (KMAC) achieves a higher capacitance than the activated carbon (KAC) derived from direct carbonization/KOH activation method in 2.0 M H_2SO_4 (315 F/g *vs.* 202 F/g) and 6.0 M KOH (251 F/g *vs.* 214 F/g) electrolyte. The present work provides a facile approach towards the fabrication of electrochemical-active oxygen functionalized porous carbon, which can be extend to the synthesis of other electrochemical-active heteroatom doped carbon and thus offers the opportunity for the practical applications of this type of carbonaceous materials in various areas such as electrochemical energy storage, catalysis and etc.

Acknowledgements

This work was financially supported by the National Science Foundation of China (20773062, 20773063, 21173119, and 21273109), the Fundamental Research Funds for the Central Universities, the Hubei Key Laboratory for Processing and Application of Catalytic Materials (CH201401), the Natural Science Fund of Hubei Province (2017CFB155), Scientific Research Plan Project of Hubei Education Department (B2017269) and Scientific Research Initial funding for the Advanced Talent of Jianghan University (1009-06810001).

Appendix A. Supplementary data

Supplementary material related to this article can be found, in the online version, at doi:https://doi.org/10.1016/j.apsusc.2017.12.142

References

[1] D. Qi, Y. Liu, Z. Liu, L. Zhang, X. Chen, 1602802, Adv. Mater. 29 (2017).
[2] K. Liang, L. Li, Y. Yang, ACS Energy Lett 2 (2017) 373.

[3] S. Khamlich, Z. Abdullaeva, J.V. Kennedy, M. Maaza, Appl. Surf. Sci. 405 (2017) 329.
[4] J. Li, M. Wei, W. Chu, N. Wang, Chem. Eng. J. 316 (2017) 277.
[5] M. Xie, S. Duan, Y. Shen, K. Fang, Y. Wang, M. Lin, X. Guo, ACS Energy Lett. 1 (2016) 814.
[6] J. Liang, L. Bu, W. Cao, T. Chen, Y.C. Cao, J. Taiwan Inst. Chem. E. 65 (2016) 584.
[7] H.A. Abdul Bashid, H.N. Lim, S. Kamaruzaman, S. Abdul Rashid, R. Yunus, N.M. Huang, C.Y. Yin, M.M. Rahman, M. Altarawneh, Z.T. Jiang, P. Alagarsamy, Nanoscale Res. Lett. 12 (2017) 246.
[8] A. Ehsani, E. Kowsari, F. BoorboorAjdari, R. Safari, H. Mohammad Shiri, J. Colloid Interf. Sci. 497 (2017) 258.
[9] Z. Tian, S. Duan, Y. Shen, M. Xie, X. Guo, Appl. Surf. Sci. 407 (2017) 463.
[10] M. Xie, Y. Xia, J. Liang, L. Chen, X. Guo, Micropor. Mesopor. Mater. 197 (2014) 237.
[11] G.P. Hao, Q. Zhang, M. Sin, F. Hippauf, L. Borchardt, E. Brunner, S. Kaskel, Chem. Mater. 28 (2016) 8715.
[12] J. Liang, S. Chen, M. Xie, Y. Wang, X. Guo, W. Ding, J. Mater. Chem. A 2 (2014) 16884.
[13] K. Sun, S. Yu, Z. Hu, Z. Li, G. Lei, Q. Xiao, Y. Ding, Electrochim. Acta 231 (2017) 417.
[14] K. Ojha, B. Kumar, A.K. Ganguli, J. Chem. Sci. 129 (2017) 397.
[15] J. Chen, X. Zhou, C. Mei, J. Xu, S. Zhou, C.-P. Wong, J. Power Sources 342 (2017) 48.
[16] A. Jain, S. Jayaraman, M. Ulaganathan, R. Balasubramanian, V. Aravindan, M.P. Srinivasan, S. Madhavi, Electrochim. Acta 228 (2017) 131.
[17] W. Tian, Q. Gao, W. Qian, ACS Sustainable Chem. Eng. 5 (2017) 1297.
[18] Z. Li, Y. Li, L. Wang, L. Cao, X. Liu, Z. Chen, D. Pan, M. Wu, Electrochim. Acta 235 (2017) 561.
[19] S. Zhang, H. Gao, M. Huang, J. Zhou, J. Alloys Compd 705 (2017) 801.
[20] J. Zhu, D. Xu, C. Wang, W. Qian, J. Guo, F. Yan, Carbon 115 (2017) 1.
[21] M. Xie, K. Fang, Y. Shen, Y. Wang, J. Liang, L. Peng, X. Guo, W. Ding, Micropor. Mesopor. Mater. 223 (2016) 114.
[22] D. Guo, C. Zheng, W. Deng, X.a. Chen, H. Wei, M. Liu, S. Huang, J. Solid State Electrochem. 21 (2017) 1165.
[23] L. Zhou, H. Cao, S. Zhu, L. Hou, C. Yuan, Green Chem. 17 (2015) 2373.
[24] J. Li, W. Liu, D. Xiao, X. Wang, Appl. Surf. Sci. 416 (2017) 918.
[25] K. Sun, S. Yu, Z. Hu, Z. Li, G. Lei, Q. Xiao, Y. Ding, Electrochim. Acta 231 (2017) 417.
[26] D. Hulicova-Jurcakova, M. Seredych, G.Q. Lu, T. Bandosz, Adv. Func. Mater. 19 (2009) 438.
[27] B.M. Anjos, J.K. McDonough, E. Perre, G.M. Brown, S.H. Overbury, Y. Gogotsi, V. Presser, Nano Energy 2 (2013) 702.
[28] Y. Ji, T. Li, L. Zhu, X. Wang, Q. Lin, Appl. Surf. Sci. 254 (2007) 506.
[29] S. Kang, J. Jian-chun, C. Dan-dan, Biomass and Bioenergy 35 (2011) 3643.
[30] T. Chen, L. Pan, T. Lu, C. Fu, D.H.C. Chua, Z. Sun, J. Mater. Chem. A 2 (2014) 1263.
[31] J. Wang, S. Kaskel, J. Mater. Chem. 22 (2012) 23710.
[32] M. Xie, J. Yang, J. Liang, X. Guo, W. Ding, Carbon 77 (2014) 215.